https://doi.org/10.17221/127/2026-PSE

Differential contributions of plant- and microbial-derived carbon to soil organic carbon under perennial and annual herbaceous species in a temperate desert grassland, Northwest China

Zexin Teng[1,2], Yuying Liu[1,2], Ümüt Halik[1,2], Jianing He[1,2]*

[1]College of Ecology and Environment, Xinjiang University, Urumqi, P.R. China
[2]Ministry of Education Key Laboratory of Oasis Ecology, Xinjiang University, Urumqi, P.R. China
**Corresponding author: halik@xju.edu.cn*

Citation: Teng Z.X., Liu Y.Y., Halik Ü., He J.N. (2026): Differential contributions of plant- and microbial-derived carbon to soil organic carbon under perennial and annual herbaceous species in a temperate desert grassland, Northwest China. Plant Soil Environ., 72: 389–402.

Abstract: Desert grasslands are critical carbon sinks in arid regions, where herbaceous species selection plays a vital role in ecosystem restoration. While plant life cycle (annual *vs.* perennial) is known to affect soil organic carbon (SOC) stocks, its influence on SOC molecular composition remains poorly understood. This study examined the accumulation and environmental drivers of plant- and microbial-derived carbon biomarkers (lignin phenols and amino sugars) across the 0–40 cm soil profile under four desert herbaceous species: perennial *Karelinia caspica* (Pall.) Less. and *Glycyrrhiza inflata* Batalin., annual *Chenopodium glaucum* L. and *Salsola lanata* (Pall.) Botsch. Plant-derived C contributed more to SOC (9–15%) than microbial-derived C (3–8%), with contributions differing significantly between plant life cycles. These differences were shaped primarily by edaphic factors: plant-derived C accumulation was mainly regulated by pH, whereas microbial-derived C was affected by labile organic carbon (LOC), elemental stoichiometry (C/N, C/P), electrical conductivity, and pH. Our results indicate that herbaceous species influence SOC sequestration through divergent plant and microbial pathways. Perennial species, especially *K. caspica* and *G. inflata*, enhance SOC storage more effectively and should be prioritised in desert grassland restoration.

Keywords: arid ecosystem; vegetation management; microbial necromass; lignin degradation

Globally, grasslands store approximately 343 Pg of soil organic carbon in the top 1 m, representing about 20% of the global soil carbon pool (Conant et al. 2017, FAO 2023). With increasing drought frequency, prolonged water scarcity has led to reduced productivity and organic carbon depletion, particularly in temperate desert grasslands. Understanding the impacts of vegetation management on soil organic carbon (SOC) stabilisation is therefore critical for improving carbon pool predictions in these vulnerable ecosystems.

Stabilised *via* divergent biogeochemical mechanisms, plant and microbial residues form persistent SOC components (Whalen et al. 2022). Lignin phenols and amino sugars – molecular indicators of plant- and microbial-derived carbon – provide a targeted approach for assessing their relative contributions to SOC. Global-scale quantitative assessments using amino sugar biomarkers indicate that microbial necromass contributes approximately 47% of soil organic carbon in grasslands and 35% in

Supported by the National Natural Science Foundation of China, Project No. 32260285, and by the Third Xinjiang Scientific Expedition and Research Program of the Ministry of Science and Technology of China, Project No. 2022xjkk0301.

https://doi.org/10.17221/127/2026-PSE

forests (Wang et al. 2021a). Furthermore, contributions of lignin phenols and amino sugars to SOC vary significantly with herbaceous species (Ao et al. 2024). Perennial herbs exhibit greater microbial residue accumulation than annual systems, with soil moisture exerting considerable influence (Li et al. 2023). Accordingly, herbaceous species composition and phenology strongly shape sequestration of both plant- and microbial-derived SOC.

Herbaceous species with varying life cycles directly influence litter deposition and underground carbon allocation, regulating microbial metabolic activities and modifying SOC stabilisation pathways (Li et al. 2023). In water-scarce desert ecosystems like the Tarim River Basin, herbaceous species exhibit divergent adaptive strategies for carbon sequestration. Rather than merely reflecting quantitative biomass differences, we hypothesise that these strategies are mechanistically linked to distinct extracellular enzymatic pathways that govern carbon partitioning (Ma et al. 2018, Yang et al. 2022). Specifically, perennials may preferentially stabilise carbon through oxidative enzymes (e.g., polyphenol oxidase, peroxidase) that modulate degradation and retention of plant-derived lignin (Luo et al. 2022). Conversely, annuals, constrained by short life cycles, might stimulate microbial-derived carbon turnover *via* hydrolytic enzymes (e.g., β-1,4-N-acetyl-glucosaminidase, β-glucosidase) (Li et al. 2023). However, the relative dominance of these pathways in shaping SOC molecular profiles across herbaceous life cycles remains unresolved.

Perennial herbaceous species are generally more beneficial for SOC accumulation under drought than annuals (Siddique et al. 2023). This advantage arises from three mechanisms: (*i*) perennials develop extensive root architectures accessing deeper soil water and stimulating microbial metabolism *via* root exudation (Li et al. 2023); (*ii*) they contain elevated lignin and cellulose that impede microbial breakdown of plant detritus, facilitating plant-derived C retention (Dai et al. 2022); and (*iii*) annuals decompose large amounts of plant residues during short life cycles, potentially accelerating decomposition of existing organic matter and triggering a positive priming effect that accelerates SOC mineralisation (Li et al. 2023).

Despite evidence affirming lignin phenols and amino sugars as effective biomarkers, the distribution patterns of plant- and microbial-derived C across different herbaceous life cycles in desert grasslands remain poorly understood. Furthermore, the mechanisms by which herbaceous life cycles govern SOC molecular profiles and the key drivers of its stabilisation have yet to be elucidated. This knowledge gap limits our understanding of SOC sequestration mechanisms and hinders the development of vegetation management strategies. Therefore, this study aims to investigate the accumulation patterns and environmental drivers of plant- and microbial-derived carbon under perennial and annual herbaceous species in a temperate desert grassland of Northwest China.

In this study, we selected four typical desert herbaceous species (*Karelinia caspia*, *Glycyrrhiza inflata*, *Chenopodium glaucum*, and *Salsola lanata*) to trace plant and microbial inputs into SOC using lignin phenols and amino sugars as biomarkers. This research aimed to: (*i*) evaluate differences in the contributions of plant- and microbial-derived C to SOC across the four species, and (*ii*) identify the key factors controlling the sequestration of carbon from both sources. We proposed the following hypotheses: (1) Perennial herbaceous species facilitate greater incorporation of both plant- and microbial-derived C into SOC compared to annual species; (2) lignin phenols and amino sugars exert a stronger effect on SOC preservation in topsoil layers due to the accumulation of aboveground litter inputs, and (3) plant-derived C accumulation is predominantly driven by soil pH through its influence on lignin preservation, whereas microbial-derived C is regulated by stoichiometric constraints (C/N, C/P) and salinity (EC) that govern microbial metabolism.

MATERIAL AND METHODS

Experiment design and soil sampling. The research was conducted in the Yingbaza section (84°15'E, 41°09'N) of the Tarim River's middle reaches within Luntai County, Xinjiang Province. The area has a temperate continental desert climate, with a mean annual temperature of 11.1 °C (range: 10.6–11.5 °C) and summer extremes reaching 43.6 °C. Mean annual precipitation is 30.1 mm (range: 17.4–42.8 mm), contrasting with potential evaporation of 2 670 mm (range: 2 429–2 910 mm) (Yusup et al. 2023). Following ecological water diversion initiatives, grassland NDVI has shown increasing trends (Wang et al. 2021b). Four representative desert herbaceous species were investigated (Figure 1): perennial *Karelinia caspica* (Pall.) Less. (PK), perennial *Glycyrrhiza inflata* Batalin. (PG), annual *Chenopodium glaucum* L. (AC), annual *Salsola lanata* (Pall.) Botsch. (AS) (Wang et al. 2016).

https://doi.org/10.17221/127/2026-PSE

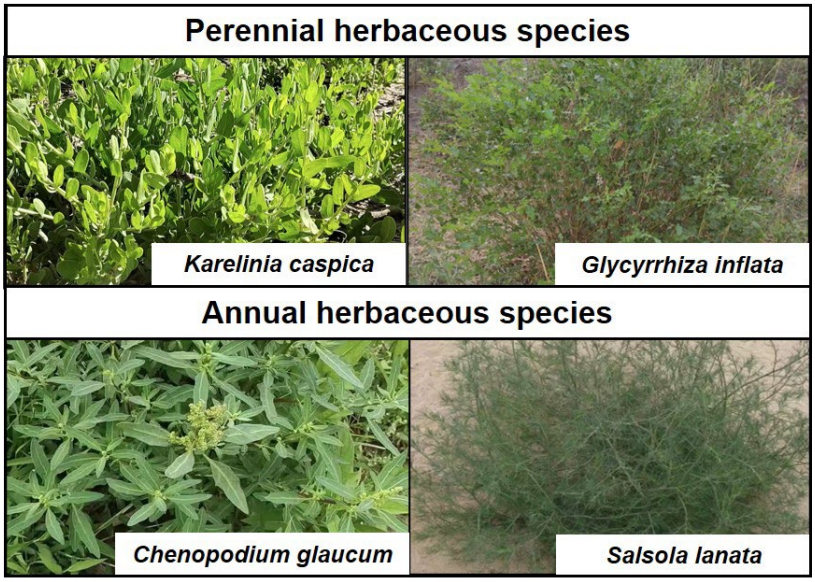

Figure 1. Images of sampling sites representing four herbaceous species

Experimental design and sample collection. In August 2024, soil samples were collected from the root zones of the four target species across four spatially distinct locations to account for soil heterogeneity (Table 1). At each location, a 5 × 5 m main quadrat was established, within which three randomly positioned 1 × 1 m subquadrats served as spatial replicates. To minimise distance-related variation, samples were collected at a standardised distance (5–10 cm) from plant bases using a stainless-steel shovel. Soils were excavated from two depths: topsoil (0–20 cm) and subsoil (20–40 cm). Samples from the three sub-quadrats at each site were homogenised to generate a representative composite sample for each depth and species.

Analysis of soil biochemistry. Soil water content (SWC) was determined gravimetrically by oven-drying fresh samples at 105 °C for 24 h. For all other analyses, soil samples were air-dried and passed through a 2 mm sieve; results are expressed on an oven-dried soil weight basis (105 °C). Soil pH was measured in a 1:5 (*w*/*v*) soil-water suspension. Electrical conductivity (EC) was determined using an EC meter. Cation exchange capacity (CEC) was quantified by the cobalt hexamine chloride method (Rhoads 1996). Soil organic carbon was analysed by potassium dichromate oxidation spectrophotometry ($K_2Cr_2O_7$-H_2SO_4) (Nelson and Sommers 1982). Total nitrogen (TN) was determined by the semi-micro Kjeldahl technique (Jackson 1958), and the ammoniacal nitrogen (NH_4^+-N) was extracted *via* the 2 mol/L KCl (Nelson and Sommers 1982). Total phosphorus (TP) was analysed by digestion followed by molybdenum antimony colourimetric detection (Parkinson and Allen 1975). Labile organic carbon (LOC) was extracted with 333 mmol/L $KMnO_4$ solution (Xu et al. 2013). Activities of phenol oxidase (POX), peroxidase (PERX), β-1,4-glucosidase (BG), and β-1,4-N-acetylglucosaminidase (NAG) were quantified using microplate-based fluorometric and spectrophotometric methods (DeForest 2009).

Analysis of lignin phenols. The lignin phenols (VSC) content consists of vanillyl (V) compounds (vanillin, acetovanillone, and vanillic acid), syringyl (S) compounds (syringaldehyde, acetosyringone, and syringic acid), and cinnamyl (C) compounds (p-coumaric acid and ferulic acid). Lignin phenols were extracted using alkaline cupric oxide oxidation

Table 1. Sampling location information

Plant life cycle	Herbaceous species	Site	Altitude (m a.s.l.)
Perennial	*Karelinia caspica* (Pall.) Less.	84°11'56.87"E, 41°16'14.70"N	919
	Glycyrrhiza inflata Batalin.	84°18'52.20"E, 41°15'12.06"N	918
Annual	*Chenopodium glaucum* L.	84°17'13.60"E, 41°15'56.84"N	924
	Salsola lanata (Pall.) Botsch.	84°17'10.32"E, 41°15'51.01"N	923

https://doi.org/10.17221/127/2026-PSE

(Hedges and Ertel 1982). Concentrations of plant-derived lignin biomarkers were normalised to SOC (mg/g SOC) to assess their relative distribution (Ma et al. 2018). The contribution of plant-derived C to SOC (%) was then calculated directly from these normalised concentrations, with 10 mg/g SOC corresponding to 1% contribution (Qin et al. 2024). Furthermore, the mass ratios of acid to aldehyde (Ad/Al) for the vanillyl (V) and syringyl (S) lignin units, denoted as $(Ad/Al)_v$ and $(Ad/Al)_s$, were calculated (Hedges and Ertel 1982, Xia et al. 2023). These ratios serve as established biogeochemical indicators of lignin degradation, with higher Ad/Al values indicating more advanced side-chain oxidation and decomposition of plant residues by soil microorganisms (Ma et al. 2020, Chen et al. 2021).

Analysis of amino sugars. Amino sugars, including glucosamine (GluN), galactosamine (GalN), mannosamine (ManN), and muramic acid (MurA), were extracted using alkaline oxidation (Zhang and Amelung 1996). After derivatisation, the concentrations of individual amino sugars were determined by gas chromatography. Total amino sugar (AS) content was calculated as the sum of GluN, GalN, ManN, and MurA. The GluN/MurA molar ratio was used to distinguish fungal- from bacterial-derived residues (Engelking et al. 2007). The calculation method for the contribution of microbial-derived C to SOC (%) was consistent with the contribution of plant-derived C to SOC (%).

Statistical analyses. All data were processed using IBM SPSS Statistics (version 26.0, IBM Corp., Armonk, USA) and presented as mean ± standard error (SE). One-way ANOVA was used to assess significant differences among herbaceous species at each soil depth. Two-way ANOVA was used to evaluate the main effects and interactions of herbaceous species and soil depth on biomarker concentrations and ratios. Tukey's post hoc test ($P < 0.05$) was used for multiple comparisons. Regression modelling examined relationships among plant- and microbial-derived C, their contributions to SOC, and edaphic factors. Correlation heatmaps were generated using the ‚corrplot' package in R (v4.2.1; CRAN, https://cran.r-project.org/package=corrplot). Redundancy analysis (RDA) was performed with CANOCO 5 to elucidate relationships between biomarker variables and soil physicochemical properties.

Table 2. The soil physicochemical properties and soil nutrients within four herbaceous species

Properties	Units	Topsoil				Subsoil			
		perennial		annual		perennial		annual	
		Karelinia caspica	*Glycyrrhiza inflata*	*Chenopodium glaucum*	*Salsola lanata*	*Karelinia caspica*	*Glycyrrhiza inflata*	*Chenopodium glaucum*	*Salsola lanata*
SWC	(%)	6.00 ± 1.58	8.18 ± 3.96	6.68 ± 0.09	15.06 ± 2.08	6.32 ± 1.06^{b}	11.04 ± 1.56^{b}	5.40 ± 0.81^{ab}	15.52 ± 1.85^{a}
pH		7.56 ± 0.04^{ab}	7.46 ± 0.08^{b}	7.70 ± 0.02^{a}	7.52 ± 0.02^{ab}	7.62 ± 0.06	7.72 ± 0.13	7.75 ± 0.06	7.45 ± 0.09
EC		1.17 ± 0.07^{ab}	1.59 ± 0.52^{ab}	0.69 ± 0.05^{b}	2.93 ± 0.46^{a}	0.56 ± 0.10^{ab}	1.02 ± 0.48^{ab}	0.45 ± 0.08^{b}	2.67 ± 0.61^{a}
CEC	($cmol_+$/kg)	6.02 ± 0.42	4.71 ± 0.23	8.11 ± 2.27	5.22 ± 1.18	5.96 ± 0.63	5.35 ± 0.39	4.84 ± 0.48	5.01 ± 0.43
TP	(g/kg)	0.68 ± 0.03	0.71 ± 0.04	0.58 ± 0.06	0.55 ± 0.01	0.65 ± 0.05	0.60 ± 0.03	0.57 ± 0.04	0.57 ± 0.01
TN	(g/kg)	0.30 ± 0.03	0.33 ± 0.10	0.23 ± 0.06	0.41 ± 0.09	0.23 ± 0.04	0.23 ± 0.05	0.19 ± 0.03	0.33 ± 0.03
NH_4^+-N	(mg/kg)	8.40 ± 1.00	8.78 ± 1.52	9.12 ± 0.46	7.01 ± 0.48	9.60 ± 0.90	10.62 ± 2.23	8.55 ± 1.08	7.16 ± 0.19
LOC	(g/kg)	0.25 ± 0.04	0.48 ± 0.016	0.32 ± 0.07	0.29 ± 0.03	0.37 ± 0.14	0.30 ± 0.10	0.21 ± 0.07	0.17 ± 0.01

Soil properties in different herbaceous species and soil depth (mean ± SE). Lowercase letters indicate different levels between the four herbaceous species ($P < 0.05$). SWC – soil water content; pH – soil pH; EC – soil electric conductivity; CEC – soil cation exchange capacity; TP – total phosphorus; NH_4^+-N – soil ammonium nitrogen; LOC – labile organic carbon. Lowercase letters (a, b, and c) in the same row indicate significant differences among herbaceous species at the 0.05 level

https://doi.org/10.17221/127/2026-PSE

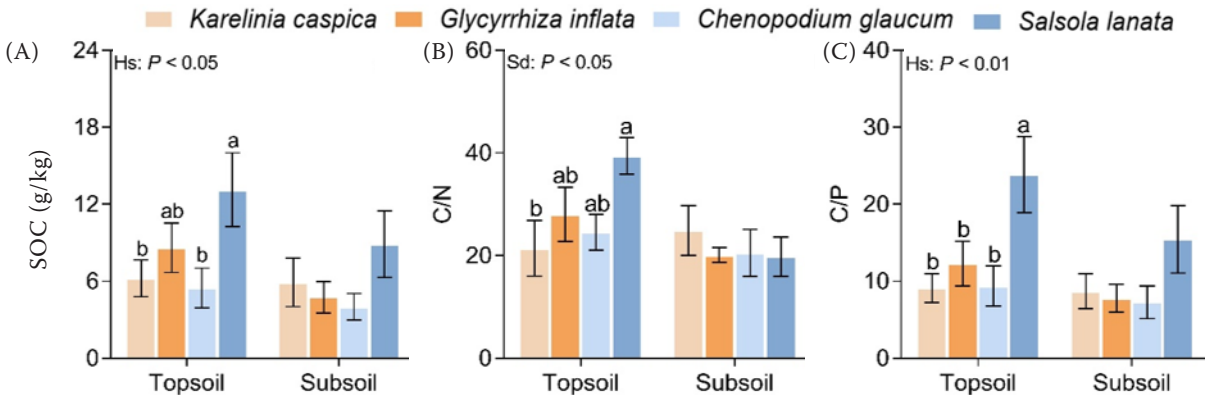

Figure 2. Soil organic carbon (SOC) content of four herbaceous species at different soil depths. C/N and C/P are the ratios of SOC to total nitrogen and total phosphorus, respectively. Significant differences ($P < 0.05$) between herbaceous species are indicated using lowercase letters. Only significant differences were labelled. The influences of herbaceous species and soil depth were evaluated through two-way ANOVA. Perennial herbaceous species: *Glycyrrhiza inflata*, *Karelinia caspica*. Annual herbaceous species: *Chenopodium glaucum*, *Salsola lanata*. Hs – herbaceous species; Sd – soil depth; Hs × Sd – interaction effect

RESULTS

Soil physicochemical attributes and enzymatic activities. Table 2 lists the soil chemical properties in different herbaceous species. Soil depth did not significantly affect these properties. In subsoil, SWC was 15.52% in AS compared to 5.40% in AC, while pH was markedly higher in AC (7.75) than in AS (7.45). Topsoil SOC was significantly determined by herbaceous species, with AS exhibiting 2.1- and 2.4-fold higher concentrations than PK and AC, respectively (Figure 2A). The C/N and C/P in the topsoil were markedly influenced by herbaceous species (Figure 2B, C). Herbaceous species effects on enzyme activities were enzyme-specific. BG activity in PG and AC was higher in topsoil than in subsoil (Figure 3D). POX activity differed significantly among herbaceous species and was highest in AS (Figure 3C).

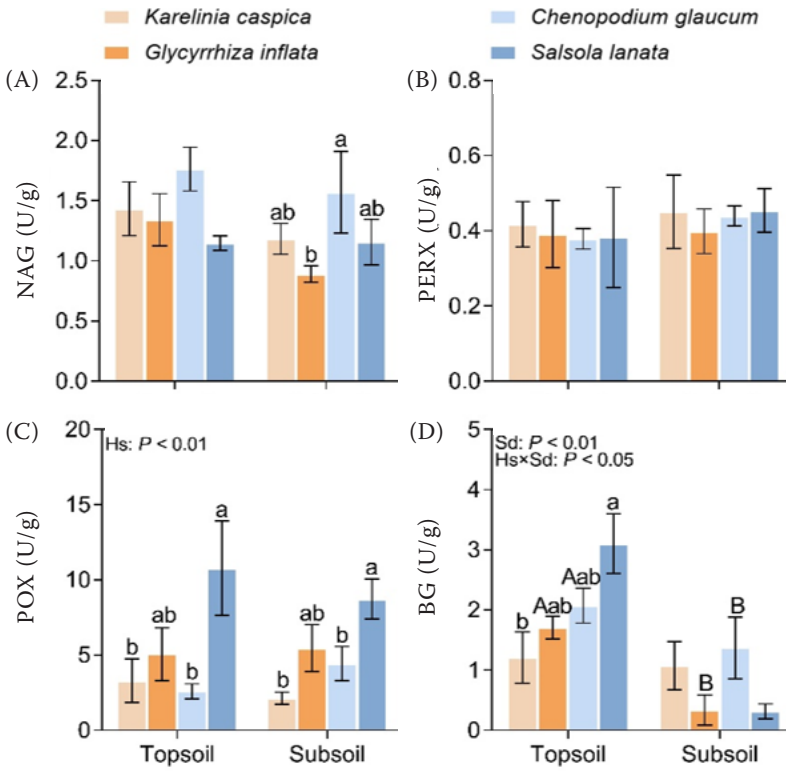

Figure 3. Soil enzyme activity of four herbaceous species in different soil depths. (A) NAG (N-acetyl-D-(+)-glucosamine); (B) PERX (peroxidase); (C) POX (polyphenol oxidase), and (D) BG (β-Glucosidase). Error bars represent the standard error of the mean ($n = 6$). Lowercase letter indicates significant difference ($P < 0.05$) among herbaceous species, and uppercase letter indicates significant difference ($P < 0.05$) among soil depths. Hs – herbaceous species; Sd – soil depth; Hs × Sd – interaction effect

https://doi.org/10.17221/127/2026-PSE

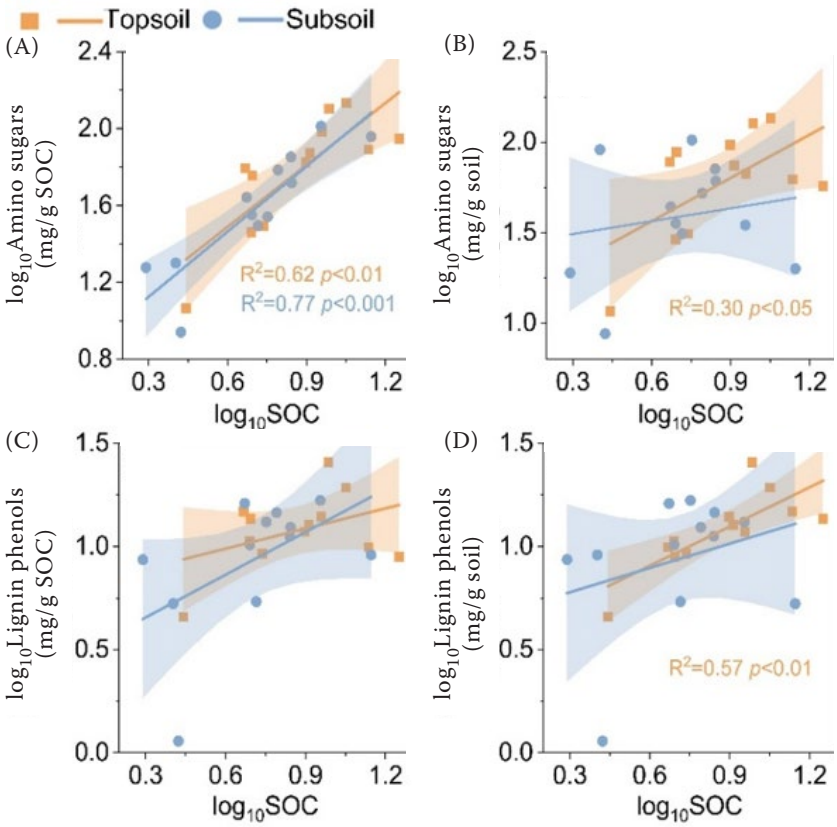

Figure 4. Associations between soil organic carbon (SOC) and the contents of lignin phenols and amino sugars. (A) and (C) show concentrations normalised per gram of SOC; (B) and (D) display values expressed per kilogram of soil

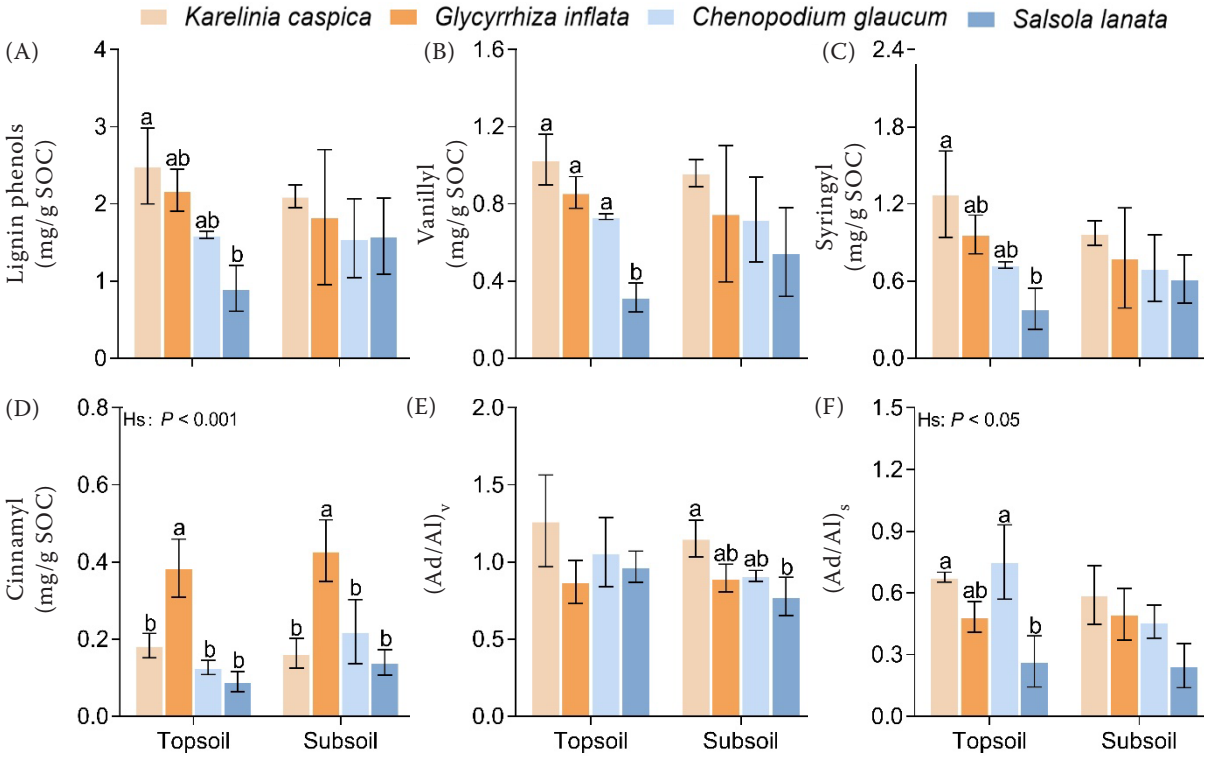

Figure 5. Soil organic carbon (SOC) normalised lignin phenol concentrations (A–D), $(Ad/Al)_s$ and $(Ad/Al)_v$ ratios (E–F) in different soil depths of the four herbaceous species. Significant differences ($P < 0.05$) between herbaceous species are indicated using lowercase letters. Only significant differences were labelled. Hs – herbaceous species; Sd – soil depth; Hs × Sd – interaction effect

https://doi.org/10.17221/127/2026-PSE

Soil lignin phenol. Lignin phenol contents in desert grassland ranged from 0.91 to 2.49 mg/g SOC (Figure 5), with vanillyl and syringyl as dominant components (Figure 5B, C). Soil depth exerted no significant influence on lignin phenol concentrations. Herbaceous species significantly altered lignin phenol concentrations in topsoil. In PK, the levels of VSC, V, and S were markedly higher than in AS (Figure 5B, C). The $(Ad/Al)_S$ was notably greater in AC than in AS (Figure 5F). Lignin phenol concentrations normalised to SOC showed a positive but non-significant correlation with SOC content (Figure 4C), whereas the lignin phenol content was significantly and positively correlated with SOC in the topsoil (Figure 4D).

Soil amino sugars. Amino sugar contents in desert grassland ranged from 6.33–11.85 mg/g SOC (Figure 6). Glucosamine and galactosamine predominated among amino sugar components (Figure 6B, C). Soil depth exerted no significant effect on amino sugar concentrations. However, herbaceous species significantly altered amino sugar concentrations. In topsoil, PK exhibited higher total amino sugars and glucosamine than AC and AS (Figure 6A, B). PG contained more galactosamine than AS in topsoil, while PK surpassed AS in subsoil galactosamine (Figure 6C). Amino sugar concentrations normalised to SOC were significantly and positively correlated with SOC content in both topsoil and subsoil (Figure 4A), whereas the absolute amino sugar content showed a significant positive correlation with SOC only in the topsoil (Figure 4B).

Assessment of the plant- and microbial-derived C. The carbon concentration from plant-derived C ranged from 60.37 ± 18.48 to 156.63 ± 26.15 mg/g SOC (Figure 7A), while that from microbial-derived C ranged from 41.24 ± 8.42 to 71.54 ± 5.67 mg/g SOC (Figure 7B). Across all herbaceous species and soil depths, the contribution of plant-derived C to SOC ranged from 6% to 16%, and that of microbial-derived C ranged from 4% to 7% (Figure 7A, B). Plant-derived C contributed more to SOC than microbial-derived C (Figure 7A, B). In the topsoil, the plant- and microbial-derived C of perennial herbaceous species were significantly higher than that of annuals (Figure 8). Among the species, PK demonstrated the highest microbial-derived C ac-

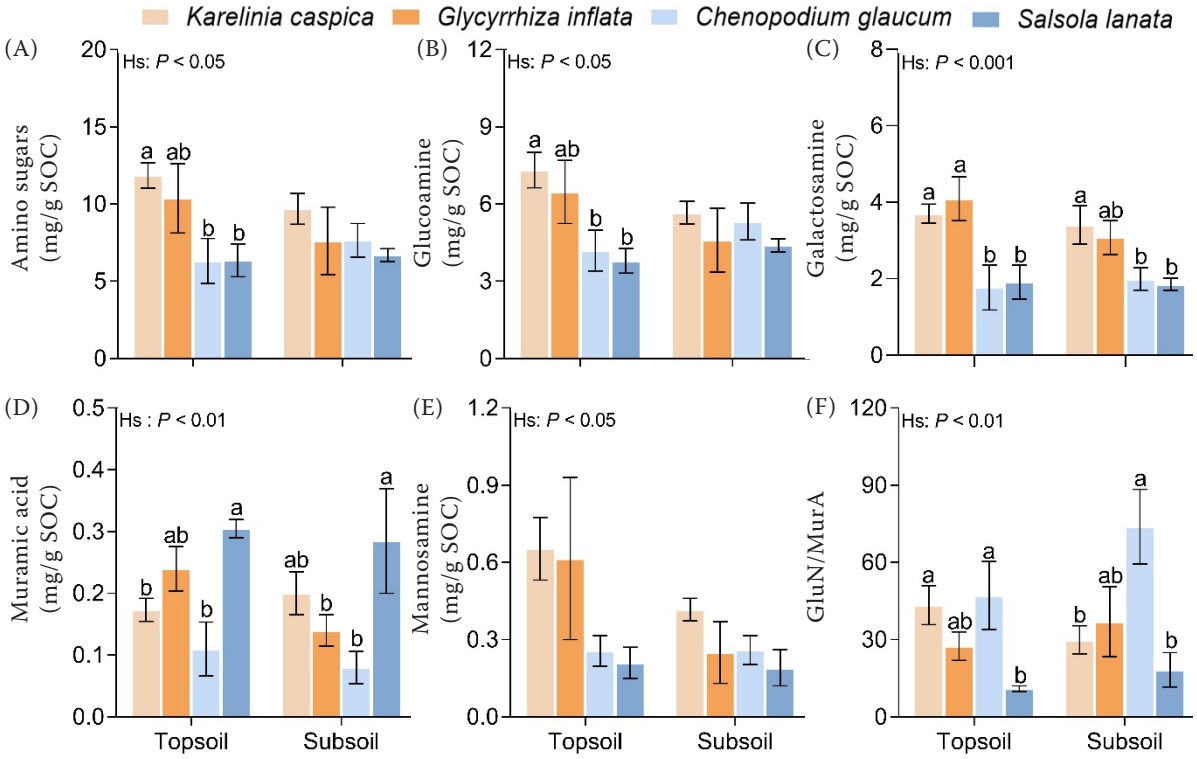

Figure 6. Soil organic carbon (SOC) normalised amino sugars concentrations (A–E) and glucosamine (GluN)/mannosamine (ManN) ratio (F) in different soil depths of the four herbaceous species. Significant differences ($P < 0.05$) between herbaceous species are indicated using lowercase letters. Only significant differences were labelled. Hs – herbaceous species; Sd – soil depth; Hs × Sd – interaction effect

https://doi.org/10.17221/127/2026-PSE

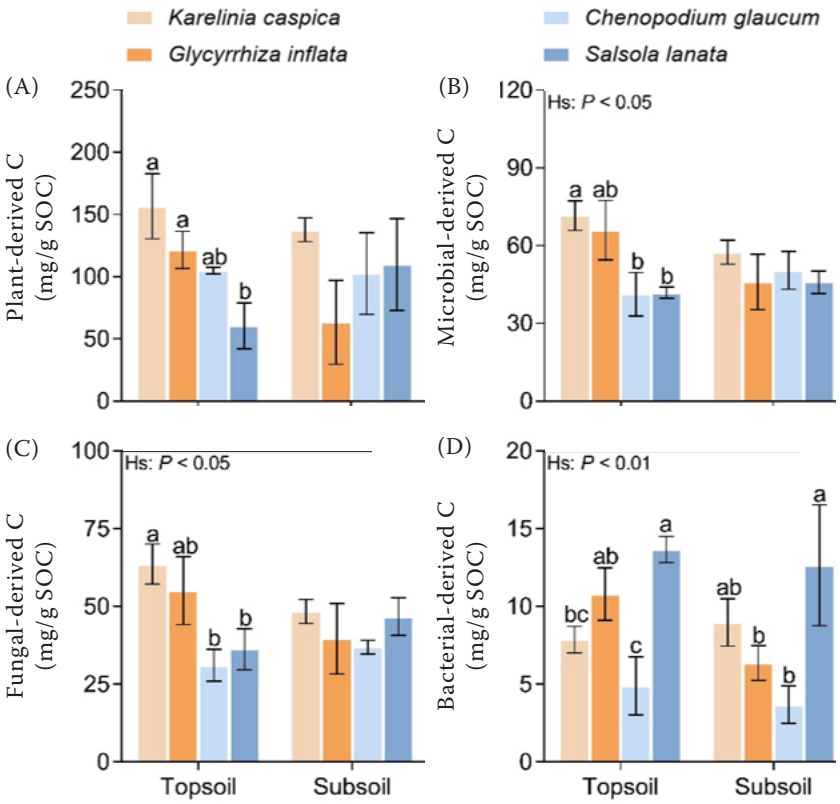

Figure 7. Soil organic carbon (SOC)-normalised concentrations of plant-derived C (A) and microbial-derived C (B–D) in different soil depths of the four herbaceous species. Significant differences ($P < 0.05$) between herbaceous species are indicated using lowercase letters. Only significant differences were labelled. Hs – herbaceous species; Sd – soil depth; Hs × Sd – interaction effect

cumulation, with fungal-derived C accounting for 89.0% of the total (Figure 7C). Both carbon fractions showed minimal vertical differentiation between topsoil and subsoil. Herbaceous species exerted significant effects on topsoil carbon pools: PK surpassed AS in plant-derived C accumulation (Figure 7A). At the same time, PK and PG exhibited elevated microbial- and fungal-derived C relative to AC and AS (Figure 7B, C). Bacterial-derived C was highest in AS across both soil depths (Figure 7D).

Relationship between soil environmental factors and soil plant- and microbial-derived C. According to the RDA results, soil properties significantly influenced the levels of lignin phenols and amino sugars (Figure 9). SOC, C/N and C/P had the longest predictions and had the greatest impact on lignin phenols and amino

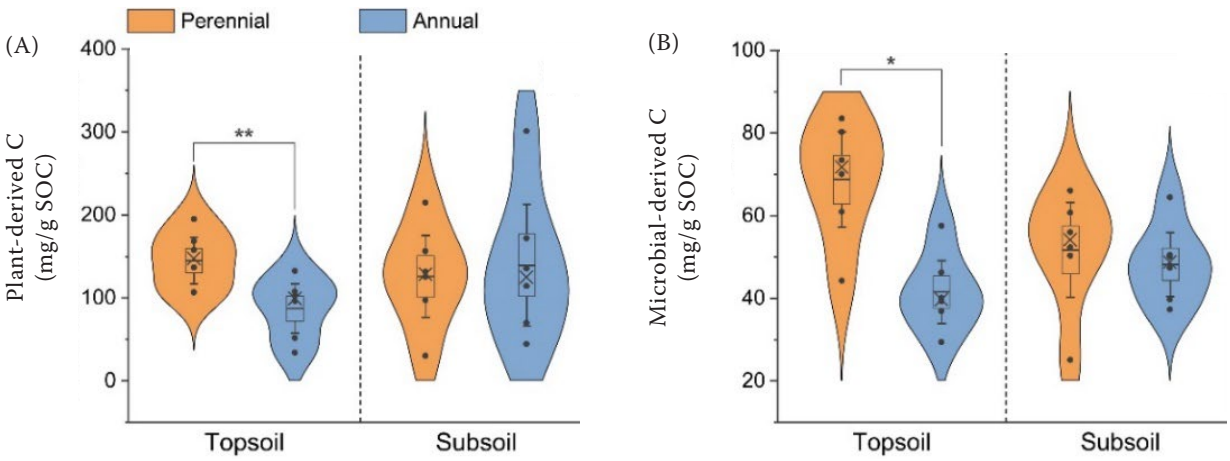

Figure 8. Soil organic carbon (SOC)-normalised levels of plant- and microbial-derived C (A, B) in the topsoil and subsoil under perennial and annual herbaceous species. The silhouette of each violin plot depicts the probability density of the data. Within the box plot, a horizontal bar and a cross represent the mean and median values for each group, respectively. Filled circles represent experimentally obtained measurements. *$P < 0.05$; **$P < 0.01$

https://doi.org/10.17221/127/2026-PSE

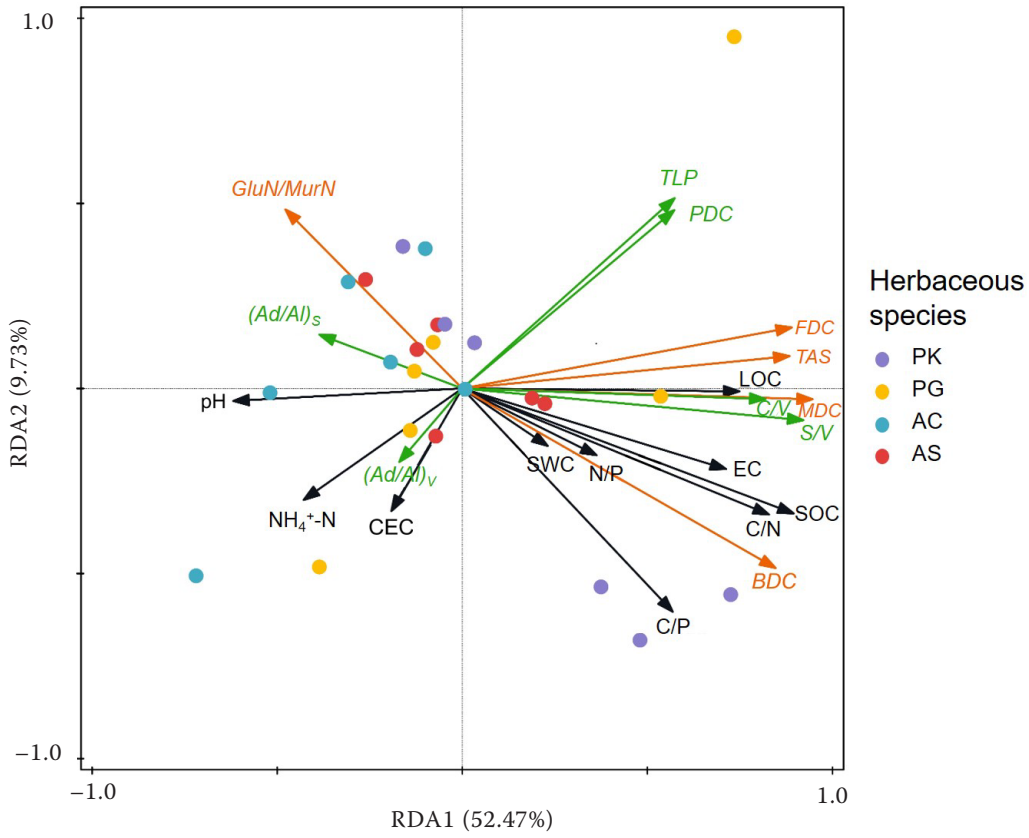

Figure 9. Redundancy analysis (RDA). It was performed to investigate the compositional patterns of two biomarker – lignin phenols (green lines) and amino sugars (orange lines) – in relation to soil properties (black lines) across both topsoil and subsoil layers. Arrows represent the correlations between the biomarkers and soil properties. PDC – plant-derived C; MDC – microbial-derived C; FDC – fungal-derived C; BDC – bacterial-derived C; SOC – soil organic carbon; TLP – total lignin phenols; TAS – total amino sugars; C/V – ratio of cinnamyl to vanillyl; S/V – ratio of syringyl to vanillyl; SWC – soil water content; SWC – soil water content; pH – soil pH; EC – soil electric conductivity; CEC – soil cation exchange capacity; NH_4^+-N – soil ammonium nitrogen; LOC – labile organic carbon; TN – total nitrogen; TP – total phosphorus; C/N – ratio of SOC to TN; C/P – ratio of SOC to TP; N/P – ratio of TN to TP

sugars. Pearson's linear correlation analysis further demonstrated statistically significant associations among plant- and microbial-derived C and key soil properties (Figure 10). Microbial-derived C showed positive correlations with EC, LOC, C/N, and C/P ratios (Figure 10C–F), but was inversely correlated with pH (Figure 10B). Plant-derived C showed negative correlations with pH (Figure 10A).

DISCUSSION

The proportional contribution of plant-derived C to SOC (6–16%) was higher than microbial-derived C (4–7%) in a temperate desert grassland. This pattern was attributed to moisture-limited microbial degradation activities in arid temperate desert soils, resulting in higher relative proportions of plant-derived C and lower microbial-derived C in SOC, as previously observed by Ma et al. (2018).

Differential contributions of plant- and microbial-derived C to SOC across herbaceous species. Consistent with Hypothesis 1, perennial herbaceous species (PK and PG) demonstrated greater incorporation of both plant-derived C (16%) and microbial-derived C (6%) into the SOC pool relative to annual species (AC and AS), which contributed 11% and 4%, respectively.

In the topsoil, perennial species accumulated more plant-derived C than annuals (Figure 8A), likely due to their dense root systems in the upper 30 cm, which may physically protect organic carbon through continuous inputs of lignin-rich root residues (Yang et al.

https://doi.org/10.17221/127/2026-PSE

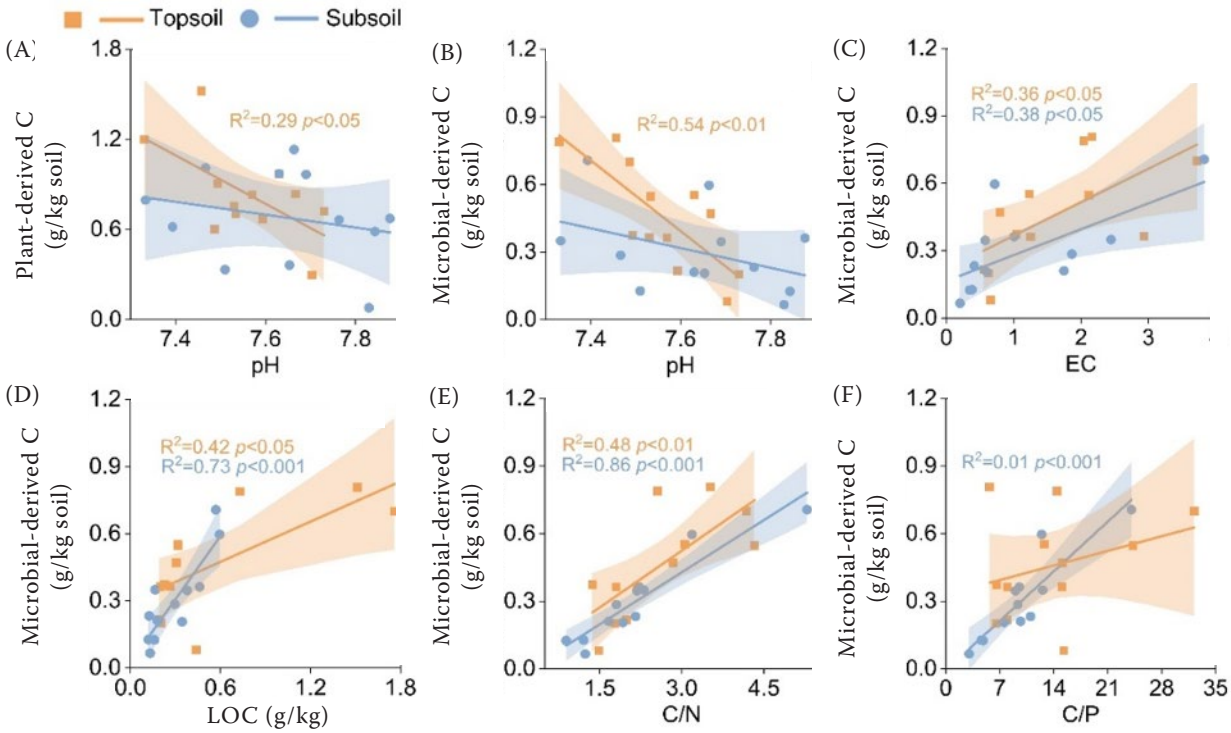

Figure 10. Analysis of regression between plant- and microbial-derived carbon (C) and soil properties. Association of plant-derived C with pH (A); depicts the associations of microbial-derived C with pH, labile organic carbon, electrical conductivity (B–F); the ratios of soil organic carbon (SOC) to total nitrogen and total phosphorus

2022). Furthermore, sustained rhizodeposition inputs (e.g., polysaccharides, organic acids) from perennials may contribute to greater soil aggregate stability than from annuals, as suggested by Baumert et al. (2018), thereby potentially protecting plant-derived organic matter from decomposition. This aligns with Yang et al. (2022), who reported 30–50% higher root inputs and reduced soil disturbance in perennial grasslands, leading to increased plant-derived C contributions. In contrast, annuals (AC and AS) have shallow roots (< 30 cm) and short life cycles, concentrating litter inputs in topsoil and accelerating microbial turnover. In the subsoil, $(Ad/Al)_V$ values were slightly lower in annual species than in perennials, with significant differences detected among species (Figure 5E). In the topsoil, $(Ad/Al)_S$ was notably greater in AC than in AS (Figure 5F), indicating species-specific variation in side-chain oxidation rather than a general pattern across all annuals (Chen et al. 2021). As a key agent in lignin decomposition, phenol oxidase (POX) promotes lignin breakdown, thereby inhibiting plant-derived C accumulation (Chen et al. 2018, Luo et al. 2022). Consistently, higher POX activity was observed in annuals (Figure 3C), suggesting greater lignin degradation capacity. This may be attributed to annuals completing their growth within a single season, resulting in litter that is lower in lignin and higher in nitrogen, making it more susceptible to rapid microbial decomposition (Li et al. 2017). Additionally, lacking deep roots and storage organs, annuals under drought stress rely more heavily on enzymatic antioxidant mechanisms such as POX for stress mitigation.

Perennial species also accumulated more microbial-derived C than annuals (Figure 8B), attributable to their deep-rooted nature. Their root systems penetrate deeper layers, maintaining water and nutrient uptake during drought. Crucially, these deep roots transport photosynthetic carbon to deeper strata with lower microbial activity, where it may undergo enhanced physicochemical stabilisation, thereby increasing long-term stability of microbial-derived C (Mou et al. 2025). In contrast, annuals rely on surface moisture; their microbial activity is more easily disrupted during drought, leading to intensified losses of carbon mineralisation in topsoil (Zhao et al. 2024). Moreover, microbial-derived C in perennials was dominated by fungal-derived C (Figure 7C), associated with higher mycorrhizal colonisation rates and diversity indices – characteristics known to pro-

https://doi.org/10.17221/127/2026-PSE

mote microbial carbon accumulation and stabilisation (Zhang et al. 2025). Annuals, however, experience disrupted carbon inputs due to short life cycles, resulting in microbial communities dominated by more fluctuating bacterial populations (Figure 7D), thereby weakening long-term accumulation of microbial-derived C (Fan et al. 2025).

Differential contributions of plant- and microbial-derived C to SOC under topsoil conditions. Consistent with Hypothesis 2, plant-derived C abundance showed a significant decline with greater soil depth (Figure 7A), whereas microbial-derived C showed minimal vertical variation (Figure 7B). This stratification primarily resulted from the concentration of root litter and rhizodeposits in topsoil across both perennial and annual species. High lignin content in topsoil promoted the formation of a recalcitrant carbon pool through enhanced physicochemical protection or aggregation (Ma et al. 2020). Limited decomposition under arid conditions further enhanced the direct stabilisation of lignin phenols, as reported in shallow-rooted systems, where clay protection combined with suppressed microbial decomposition accounted for 58% of surface SOC from lignin phenols (Yusup et al. 2023). While we did not directly quantify clay mineralogy in the present study, this previous finding supports the possibility that similar mechanisms may be relevant in our desert grassland.

Lignin phenols, as molecular indicators of plant-derived C, were detected at higher concentrations in topsoil and showed a significant positive association with SOC ($P < 0.01$; Figure 4D). This trend may be attributed to constraints on microbial decomposition due to limited moisture availability in topsoil (Figure 7A). Given that lignin degradation depends on fungal-secreted oxidases (e.g., POX) whose synthesis requires adequate moisture (Ma et al. 2018), the observed lower topsoil water content creates unfavourable conditions for decomposition (Table 2). Additionally, herbaceous plants continuously deposit lignin-rich organic matter into topsoil *via* root exudates, litterfall, and fine-root turnover.

Amino sugars, as tracers of microbial-derived C, showed marked positive associations with SOC across both soil depths, with a stronger correlation in the subsoil ($P < 0.001$; Figure 4A). This pattern suggests more effective physical protection mechanisms at deeper layers, where limited oxygen availability and diminished microbial activity could facilitate long-term stabilisation of microbial residues *via* organo-mineral association and aggregate occlusion (He et al. 2024).

BG, a key enzyme hydrolysing cellobiose to glucose, was significantly higher in topsoil than in subsoil. This likely reflects the preferential decomposition of labile cellulose and hemicellulose in topsoil, releasing soluble carbon for microbial utilisation while reducing the co-metabolic demand on recalcitrant lignin, thereby indirectly preserving plant-derived C (He et al. 2022). Concurrently, drought-induced suppression of microbial activity further limits enzymatic degradation of plant residues, enhancing plant-derived C enrichment in topsoil (Yang et al. 2022).

Factors governing the formation of plant- and microbial-derived C. Redundancy analysis, heatmap visualisation, and correlation assessments identified distinct environmental drivers governing plant- and microbial-derived C incorporation into SOC. C/N, C/P, pH, and extracellular enzyme activities governed these processes (Figures 9 and 10), confirming established soil carbon stabilisation frameworks (Chen et al. 2021).

Microbial-derived C exhibited marked positive relationships with C/N and C/P (Figure 10E, F). Elevated C/P ratios typically indicate phosphorus limitation, under which microorganisms enhance carbon assimilation efficiency and allocate more resources to microbial residue synthesis (Tao et al. 2023). Similarly, in high C/N desert soils, fungal-derived C was relatively high (Figure 9), reflecting fungi's superior carbon use efficiency in forming stable microbial-derived pools (Yu et al. 2025). EC demonstrated a significant positive correlation with microbial-derived C (Figure 10D). This is consistent with Rath and Rousk (2015), who reported that under salinised conditions (EC > 0.2), microbial communities produce compatible solutes (e.g., glycerol, proline, betaine), which contribute to microbial-derived C pools following cellular mortality.

While neutral-to-alkaline pH typically enhances plant-derived C preservation in non-saline soils through fungal-mediated mineral associations (Malik et al. 2018), our data demonstrate the opposite effect in arid saline-alkali systems. Elevated pH reduced plant-derived C through dual mechanisms (Figure 10A). First, high pH inhibited lignin-degrading fungal communities, accelerating mineralisation of labile carbon pools (Yang et al. 2022). Second, alkaline conditions are known to alter clay surface chemistry and compromise aggregate stability, thereby weakening mineral protection of plant residues (Shen et al. 2024). Although we did not directly measure these structural properties, this mechanism provides

https://doi.org/10.17221/127/2026-PSE

a plausible explanation for the negative effect of high pH on plant-derived C retention observed in our study. These processes disrupted the equilibrium between carbon input and stabilisation, ultimately diminishing plant-derived C retention. Notably, pH also had negative effects on microbial-derived C, likely due to alkaline suppression of acidophilic fungal activity (Figure 10B; Rousk et al. 2010). Although pH-tolerant Actinobacteria dominated under these conditions, their necromass exhibited lower chemical stability than fungal necromass, thereby reducing microbial carbon accumulation rates (Chen et al. 2021). This creates a self-reinforcing depletion cycle where impaired stabilisation synergistically reduces both plant- and microbial-derived C pools in saline-alkali ecosystems.

In conclusion, this study demonstrates that herbaceous species play a critical role in regulating the incorporation of plant- and microbial-derived carbon into SOC in temperate desert grasslands. Across all species examined, plant-derived C was the dominant contributor to SOC pools, confirming that plant residues constitute a major fraction of SOC in arid ecosystems. Perennial herbaceous species exhibited a significantly greater capacity to sequester both plant- and microbial-derived C than annual species, particularly in topsoil (0–20 cm), where distinct vertical stratification in SOC stabilisation mechanisms was observed. The incorporation of these carbon pools was primarily governed by C/N, C/P, pH, and extracellular enzyme activities.

These findings have important implications for ecosystem restoration. Given the central role of plant- and microbial-derived C in SOC formation, future efforts should focus on understanding SOC preservation mechanisms under perennial herbaceous species. Prioritising perennial herbs in restoration plans is strongly recommended to enhance carbon sequestration, improve soil health, and bolster ecosystem resilience. This study provides a scientific framework for developing species-specific management strategies to optimise soil carbon storage and ecosystem recovery in temperate desert grasslands.

Limitations and future directions. Several limitations of this study should be acknowledged. First, biomarker assessments were conducted on bulk soils, which cannot differentiate specific physical fractions (e.g., particulate *vs.* mineral-associated organic matter). Consequently, discussions regarding mineral-organic complexation remain inferential due to the absence of quantitative soil mineralogy and texture data. Moreover, we did not directly quantify soil structural properties such as aggregate size distribution or soil texture. Therefore, inferences regarding the physical protection of SOC (e.g., *via* aggregate occlusion or organo-mineral association) remain speculative and require confirmation in future studies integrating physical fractionation techniques and detailed soil mineralogical analyses. Second, while extracellular enzyme activities reflect carbon turnover potential, the lack of microbial biomass or metagenomic data limits our ability to normalise these activities and link them directly to specific microbial communities. Future studies integrating physical fractionation techniques and high-throughput sequencing would provide a more comprehensive understanding of SOC formation and stabilisation mechanisms under different herbaceous species.

Acknowledgement. We thank Yuying Liu for her valuable help with Investigation, Methodology, Writing – review and editing. We thank Ümüt Halik for his valuable help with Conceptualisation, Data curation, Writing – Review and editing, Supervision and Funding acquisition. We thank Jianing He for his valuable help with the investigation.

REFERENCES

Ao D., Wang B., Wang Y., Chen Y., Anum R., Feng C., Ji M., Liang C., An S. (2024): Grassland degraded patchiness reduces microbial necromass content but increases contribution to soil organic carbon accumulation. Science of the Total Environment, 951: 175717.

Baumert V., Vasilyeva N.A., Vladimirov A.A., Meier I.C., Kögel-Knabner I., Mueller C.W. (2018): Root exudates induce soil macroaggregation facilitated by fungi in subsoil. Frontiers in Environmental Science, 6: 140.

Chen J., Luo Y., van Groenigen K.J., Hungate B.A. (2018): A keystone microbial enzyme for nitrogen control of soil carbon storage. Science Advances, 4: eaaq1689.

Chen X., Hu Y., Xia Y., Zheng S., Ma C., Rui Y., He H., Huang D., Zhang Z., Ge T., Wu J., Wang Y., Su Y. (2021): Contrasting pathways of carbon sequestration in paddy and upland soils. Global Change Biology, 27: 2478–2490.

Conant R.T., Cerri C.E.P., Osborne B.B., Paustian K. (2017): Grassland management impacts on soil carbon stocks: a new synthesis. Ecological Applications, 27: 662–668.

Dai G.H., Zhu S.S., Cai Y., Zhu E.X., Jia Y.F., Ji C.J., Tang Z.Y., Fang J.Y., Feng X.J. (2022): Plant-derived lipids play a crucial role in forest soil carbon accumulation. Soil Biology and Biochemistry, 168: 108645.

https://doi.org/10.17221/127/2026-PSE

DeForest J.L. (2009): The influence of time, storage temperature, and substrate age on potential soil enzyme activity in acidic forest soils using MUB-linked substrates and L-DOPA. Soil Biology and Biochemistry, 41: 1180–1186.

Engelking B., Flessa H., Joergensen R.G. (2007): Shifts in amino sugar and ergosterol contents after addition of sucrose and cellulose to soil. Soil Biology and Biochemistry, 39: 2111–2118.

Fan J.W., Mickan B.S., Solaiman Z.M., Chen Y., Du Y.L., Abbott L.K. (2025): Microbial changes induced by defoliation: stronger associations with root traits than soil properties in annual ryegrass. Journal of Environmental Management, 391: 126432.

FAO (2023): Global Assessment of Soil Carbon in Grasslands: From Current Stock Estimates to Sequestration Potential. Rome, Food and Agriculture Organisation of the United Nations.

He J., Nie Y., Tan X., Li D., Wang K. (2024): Latitudinal patterns and drivers of plant lignin and microbial necromass accumulation in forest soils: disentangling microbial and abiotic controls. Soil Biology and Biochemistry, 194: 109438.

He M., Fang K., Chen L., Wang J., Wu Y., Yang Y., Wang A., Qin S., Chen L., Hu J., Yang Y. (2022): Depth-dependent drivers of soil microbial necromass carbon across Tibetan alpine grasslands. Global Change Biology, 28: 936–949.

Hedges J.I., Ertel J.R. (1982): Characterization of lignin by gas capillary chromatography of cupric oxide oxidation products. Analytical Chemistry, 54: 174–178.

Jackson M.L. (1958): Soil Chemical Analysis. Englewood Cliffs, Prentice Hall.

Li W.W., Du F., Zhang X.Y., Zhang B.B., Zhou M. (2017): Response of reactive oxygen scavenging enzymes among nine co-existing species in Loess Plateau to water deficit. Acta Botanica Boreali-Occidentalia Sinica, 37: 1145–1154.

Li N., Zhao N., Xu S., Wang Y., Wei L., Zhang Q., Guo T., Wang X. (2023): Accumulation of microbial necromass carbon and its contribution to soil organic carbon in artificial grasslands of various vegetation types. European Journal of Soil Biology, 119: 103573.

Luo R., Kuzyakov Y., Zhu B., Guo S., Liu S., Wang Z., Han X. (2022): Phosphorus addition decreases plant lignin but increases microbial necromass contribution to soil organic carbon in a subalpine forest. Global Change Biology, 28: 4194–4210.

Ma T., Dai G., Zhu S., Chen D., Li W., Wang B., Fu X., Wang Z., Feng X. (2020): Vertical variations in plant- and microbial-derived carbon components in grassland soils. Plant and Soil, 446: 441–455.

Ma T., Zhu S., Wang Z., Chen D., Dai G., Feng X. (2018): Divergent accumulation of microbial necromass and plant lignin components in grassland soils. Nature Communications, 9: 3480.

Malik A.A., Puissant J., Buckeridge K.M., Goodall T., Jehmlich N., Chowdhury S., Gweon H.S., Peyton J.M., Mason K.E., van Agtmaal M., Blaud A., Clark I.M., Whitaker J., Pywell R.F., Ostle N., Gleixner G., Griffiths R.I. (2018): Land use driven change in soil pH affects microbial carbon cycling processes. Nature Communications, 9: 3591.

Mou X., Li Y., Wang X., Chen Y., Li Z., Wang Y., Zhang K., Ma W., Niu K. (2025): Plant species richness mediates the responses of microbial necromass carbon accumulation to climate aridity in alpine meadows. Journal of Ecology, 113: 883–895.

Nelson D.W., Sommers L.E. (1982): Total carbon, organic carbon and organic matter. In: Page A.L., Miller R.H., Keeney D.R. (eds.): Methods of Soil Analysis. Part 2: Chemical and Microbiological Properties. Madison, SSSA, 539–579.

Parkinson J.A., Allen S. (1975): A wet oxidation procedure suitable for the determination of nitrogen and mineral nutrients in biological material. Communications in Soil Science and Plant Analysis, 6: 1–11.

Qin H., Liu Y., Chen C., Chen A., Liang Y., Cornell C.R., Guo X., Bai E., Hou H., Wang D., Zhang L., Wang J., Yao D., Wei X., Zhou J., Tan Z., Zhu B. (2024): Differential contribution of microbial and plant-derived organic matter to soil organic carbon sequestration over two decades of natural revegetation and cropping. Science of The Total Environment, 949: 174960.

Rath K.M., Rousk J. (2015): Salt effects on the soil microbial decomposer community and their role in organic carbon cycling: a review. Soil Biology and Biochemistry, 81: 108–123.

Rhoads J.D. (1996): Salinity: electrical conductivity and total dissolved solids. In: Sparks D.L. (ed.): Methods of Soil Analysis. Part 3. Chemical Methods. Madison, SSSA and ASA, 417–435.

Rousk J., Bååth E., Brookes P.C., Lauber C.L., Lozupone C., Caporaso J.G., Knight R., Fierer N. (2010): Soil bacterial and fungal communities across a pH gradient in an arable soil. The ISME Journal, 4: 1340–1351.

Shen Z., Han T., Huang J., Zhang Y., Li D., Wang B., Liu K., Feng H., Yu Q., He H., Zhang X. (2024): Soil organic carbon regulation by pH in acidic red soil subjected to long-term liming and straw incorporation. Journal of Environmental Management, 367: 122063.

Siddique I.A., Grados D., Chen J., Lærke P.E., Jørgensen U. (2023): Soil organic carbon stock change following perennialization: a meta-analysis. Agronomy for Sustainable Development, 43: 58.

Tao F., Huang Y., Hungate B.A., Manzoni S., Frey S.D., Schmidt M.W.I., Reichstein M., Carvalhais N., Ciais P., Jiang L., Lehmann J., Wang Y.P., Houlton B.Z., Ahrens B., Mishra U. (2023): Microbial carbon use efficiency promotes global soil carbon storage. Nature, 618: 981–985.

Wang B., An S., Liang C., Liu Y., Kuzyakov Y. (2021a): Microbial necromass as the source of soil organic carbon in global ecosystems. Soil Biology and Biochemistry, 162: 108422.

Wang S.S., Wang J.L., Zhou K.F., Fan Z., Wang Y. (2021b): Response of land-use/land cover change to ecological water conveyance in the lower reach of Tarim River. Water Resources Protection, 37: 69–74.

Wang X., Xu H., Pan C., Zhang J., Chen Y. (2016): Relation of dominant herbaceous plant species to groundwater depth in the lower reaches of Tarim River. Journal of Desert Research, 36: 216–224.

https://doi.org/10.17221/127/2026-PSE

Whalen E.D., Grandy A.S., Sokol N.W., Snajdr J., Baldrian P., Litton C.M. (2022): Clarifying the evidence for microbial- and plant-derived soil organic matter, and the path toward a more quantitative understanding. Global Change Biology, 28: 7167–7185.

Xia S., Song Z., Wang W., Wang H., Liu X., Li Z., Wu Y., Liu C., Wu Y., Xu S., Xu X., Xu C., Xu J., Xu Z. (2023): Patterns and determinants of plant-derived lignin phenols in coastal wetlands: implications for organic C accumulation. Functional Ecology, 37: 1067–1081.

Xu X., Thornton P.E., Post W.M. (2013): A global analysis of soil microbial biomass carbon, nitrogen and phosphorus in terrestrial ecosystems. Global Ecology and Biogeography, 22: 737–749.

Yang Y., Dou Y., Wang B., Xue Z., Wang Y., An S., Chang S.X. (2022): Increasing contribution of microbial residues to soil organic carbon in grassland restoration chronosequence. Soil Biology and Biochemistry, 170: 108688.

Yu Y., Li L., Yang J., Xu Y., Virk A.L., Zhou J., Li F.-M., Yang H., Kan Z.-R. (2025): Global synthesis on the responses of microbial- and plant-derived carbon to conservation tillage. Plant and Soil, 513: 1971–1985.

Yusup A., Halik Ü., Keyimu M., Aishan T. (2023): Trunk volume estimation of irregular shaped *Populus euphratica* riparian forest using TLS point cloud data and multivariate prediction models. Forest Ecosystems, 10: 100138.

Zhang X., Amelung W. (1996): Gas chromatographic determination of muramic acid, glucosamine, mannosamine, and galactosamine in soils. Soil Biology and Biochemistry, 28: 1201–1206.

Zhang X., Liu Y., Mo X., Li H., Li J., Wang C. (2025): Ectomycorrhizal fungi and biochar promote soil recalcitrant carbon increases under arsenic stress. Journal of Hazardous Materials, 489: 137598.

Zhao Y., Wang X., Li Y., Yang Y., An S., Chen Y. (2024): Aridity-driven divergence in soil microbial necromass carbon in alpine grasslands of the Tibetan Plateau. Biology and Fertility of Soils, 60: 799–812.

Received: March 31, 2026
Accepted: June 10, 2026
Published online: June 30, 2026